

Technical University of Denmark



Synchrotron X-ray measurement of residual strain within the nose of a worn manganese steel railway crossing

Dhar, Subash; Zhang, Yubin; Xu, Ruichao; Danielsen, Hilmar Kjartansson; Juul Jensen, Dorte

Published in:

I O P Conference Series: Materials Science and Engineering

Link to article, DOI:

[10.1088/1757-899X/219/1/012016](https://doi.org/10.1088/1757-899X/219/1/012016)

Publication date:

2017

Document Version

Publisher's PDF, also known as Version of record

[Link back to DTU Orbit](#)

Citation (APA):

Dhar, S., Zhang, Y., Xu, R., Danielsen, H. K., & Juul Jensen, D. (2017). Synchrotron X-ray measurement of residual strain within the nose of a worn manganese steel railway crossing. I O P Conference Series: Materials Science and Engineering, 219. DOI: 10.1088/1757-899X/219/1/012016

DTU Library

Technical Information Center of Denmark

General rights

Copyright and moral rights for the publications made accessible in the public portal are retained by the authors and/or other copyright owners and it is a condition of accessing publications that users recognise and abide by the legal requirements associated with these rights.

- Users may download and print one copy of any publication from the public portal for the purpose of private study or research.
- You may not further distribute the material or use it for any profit-making activity or commercial gain
- You may freely distribute the URL identifying the publication in the public portal

If you believe that this document breaches copyright please contact us providing details, and we will remove access to the work immediately and investigate your claim.

PAPER • OPEN ACCESS

Synchrotron X-ray measurement of residual strain within the nose of a worn manganese steel railway crossing

To cite this article: S Dhar *et al* 2017 *IOP Conf. Ser.: Mater. Sci. Eng.* **219** 012016

View the [article online](#) for updates and enhancements.

Related content

- [On-line 2D monitoring of rolling contact fatigue/wear phenomena in dry tests](#)
I. Bordini, C. Petrogalli, A. Mazzù et al.
- [The Simulation of Point Contact Stress State for APS Coatings](#)
D Chicet, A Tufescu, C Paulin et al.
- [Critical plane analysis of multiaxial fatigue experiments leading to White Etching Crack formation](#)
S Averbek and E Kerscher

Synchrotron X-ray measurement of residual strain within the nose of a worn manganese steel railway crossing

S Dhar¹, Y Zhang¹, R Xu², HK Danielsen¹ and D Juul Jensen¹

¹ Section for Materials Science and Advanced Characterization, Department of Wind Energy, Technical University of Denmark, Risø Campus, Roskilde, DK- 4000, Denmark

² Advanced Photon Source, Argonne National Laboratory, Argonne, IL, 60439-4800, USA

E-mail: sodh@dtu.dk, yubz@dtu.dk

Abstract. Switches and crossings are an integral part of any railway network. Plastic deformation associated with wear and rolling contact fatigue due to repeated passage of trains cause severe damage leading to the formation of surface and sub-surface cracks which ultimately may result in rail failure. Knowledge of the internal stress distribution adds to the understanding of crack propagation and may thus help to prevent catastrophic rail failures. In this work, the residual strains inside the bulk of a damaged nose of a manganese railway crossing that was in service for five years has been investigated by using differential aperture synchrotron X-ray diffraction. The main purpose of this paper is to describe how this method allows non-destructive measurement of residual strains in selected local volumes in the bulk of the rail. Measurements were conducted on the transverse surface at a position about 6.5 mm from the rail running surface of a crossing nose. The results revealed the presence of significant compressive residual strains along the running direction of the rail.

1. Introduction

Switches and crossings (S&Cs) are of great importance for any railway network as they allow trains to be directed from one track to another. The geometry, as well as the loading situations, in the nose of a crossing (see figure 1) differs from that of normal rails. It has been observed that the majority of track problems are associated with switches and crossings, which leads to higher maintenance costs than for any other part of the track. Previous studies performed on the deformation behavior of the crossing nose [1-5] clearly indicate that a very high contact stress occurs at the rail/wheel contact surface due to repeated passage of wheels. The stress levels are higher than the yield strength of the rail material, causing plastic deformation of the rail. The rail in the nose region is also subject to contact friction, and impact stresses, which lead to wear and rolling contact fatigue. Many defects can appear, including surface and subsurface cracks. The stress distribution (of both contact and residual stresses) plays an important role in generation of cracks in the material that may lead to failure. Residual stresses are generated in a rail during manufacturing as well as while in service. There are quite a few studies on the measurement of residual stresses in normal rail heads in the literature, including both modelling and experimental work [6-15]. Mostly tensile residual stresses are present in the rail head



after the straightening process during manufacturing, however in service the stress state changes due to the variable loading situations resulting in the generation of a complex stress field.

There are several different experimental techniques to measure the residual stress in any material. Non-destructive methods include the use of X-rays or neutrons. However, ordinary X-rays are limited in terms of intensity and penetration depth. This means they typically give a mean stress averaged over a penetration depth only within a small area. In recent years, neutron diffraction has been used to determine residual stresses in the rail head [8-11]. Neutrons have a significantly larger penetration depth compared to ordinary X-rays, but due to their relative low intensity only stresses averaged over fairly large volumes in the mm³-cm³ range can be determined. Alternatively, with the advent of high energy synchrotron radiation techniques, local residual stresses can be determined in the bulk of the samples. Measurements of residual stresses on worn rails [12-14] as well as roller-straightened new rail heads [15] using synchrotron X-ray diffraction method have been published.

The novelty of the present work is that we focus on strains in the heavily loaded nose of an S&C, and that the selected S&C is made of manganese steel, optimized to improve wear and fatigue resistance compared to conventional pearlitic steel. Moreover the manufacturing process of manganese steel railway crossings is different from normal rails. Specifically, they are cast as a single piece and then explosion hardened.

The purpose of this work is therefore to apply synchrotron X-ray measurements to the nose of a rail crossing, and to determine the depth profiles of the residual strains. The crossing rail sample used in the experiment was taken from the rail network after being in service for five years on a major railway line in Denmark, carrying both freight and passenger trains.

2. Experimental Procedure

The residual strains in the nose of manganese steel crossing were investigated in this study. Visual inspection of the nose revealed severe damage with cracks and spallation. The chemical composition and mechanical properties of the steel are given in table 1 and table 2, respectively. The sampling area of the nose for synchrotron measurements is described in figure 1. The slice for the measurement was 5 mm thick and strain measurements were made on the transverse surface at various depths along the longitudinal direction. To avoid mechanical strains induced during grinding and cutting of the slice, the free surface was electropolished before measurements.

Table 1. Chemical composition of the manganese steel (wt%).

C	Mn	Si	Cr	P	S	Fe
1.14	12.81	0.26	0.12	0.05	0.05	balance

Table 2. Mechanical properties of the manganese steel.

Tensile strength	Yield Strength	Elongation	Hardness
~750 MPa	~365 MPa	~20%	~220 HV

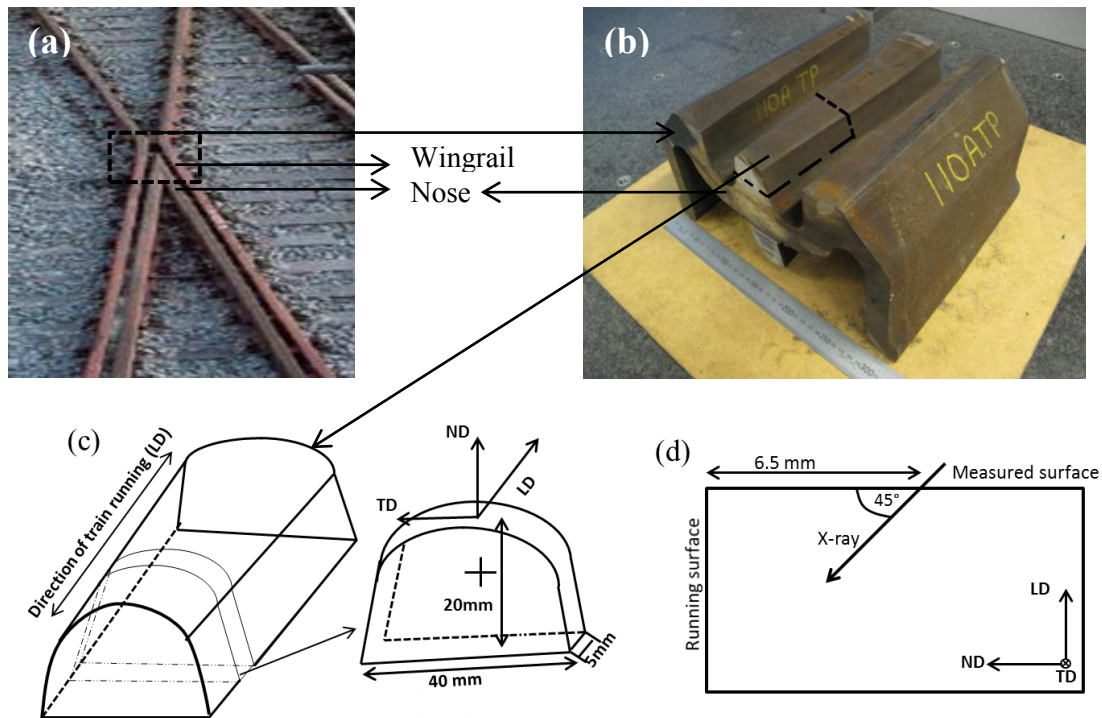


Figure 1. Nose specimen used for the synchrotron strain measurement: (a) photograph of typical crossing (with nose and wingrail); (b) part of a manganese steel crossing cut out from the track for investigation; (c) schematic showing the final sampling slice for strain measurements indicating also the normal direction (ND), transverse direction (TD) and longitudinal direction (LD). The black cross marks the position for synchrotron measurements. (d) Sketch showing the experimental set-up for the synchrotron measurements.

Synchrotron measurements were conducted on the transverse section at a position about 6.5 mm from the rail running surface of the crossing nose (see figure 1d) at beam line 34-ID-E at the Advanced Photon Source (APS), Argonne National Laboratory [16].

A focused polychromatic beam was first used to determine the orientations of the matrix grains. The use of non-dispersive Kirkpatrick-Baez (K-B) focusing mirrors helps in focusing of the beam on to the specimen. The resulting microbeam had a full-width half maximum of $\sim 0.5 \mu\text{m}$. The X-ray microbeam was scanned over the specimen, which was mounted on a holder at an inclination of 45° to the incoming beam (see figure 1d). The Laue diffraction patterns from the polychromatic scans were recorded on an area detector mounted in 90° reflection geometry 510.3 mm above the specimen. Diffraction patterns from different depths were obtained by the use of a Pt-wire of $100 \mu\text{m}$ diameter as a differential aperture. The Laue patterns at each depth were reconstructed by the use of the LaueGo software [17] available at APS beamline 34-ID-E. The patterns were indexed, from which the (hkl) indices of individual spots as well as their corresponding X-ray energies were determined. From these data, a spot with high intensity and its corresponding plane parallel to the specimen surface was selected for monochromatic energy scanning to determine the absolute lattice spacing. Thereby the strain (in one direction) was measured as:

$$\varepsilon = \frac{d-d_0}{d_0}, \quad (1)$$

where d is the lattice spacing of the sample and d_0 is the lattice spacing of the sample in the stress-free state. For the present study, d_0 was determined based on the lattice parameter measured at the base of the nose (at a depth of 20 mm from the running surface) using laboratory X-ray measurements

assuming that, apart from manufacturing stresses, this location is free from stresses induced due to wheel-rail interactions. These measurements were done at the Department of Materials and Manufacturing Technology at Chalmers University of Technology, Sweden. A chromium source (X-ray wavelength $\lambda = 2.2897 \text{ \AA}$) was used. The lattice parameter determined from the (220) peak at a diffraction angle of 126.85° is $a = 3.621 \text{ \AA}$, which is used for to obtain the reference d_0 value.

3. Results and Discussion

The crystallographic orientations measured using polychromatic beam differential aperture X-ray diffraction (DAXM) at four locations, 0.5 mm apart, are shown in figure 2. The grain orientations within a depth of 0-50 μm from the measurement surface are shown. The result shows that the grain at a position of 6.5 mm from the running surface has the smallest orientation spread (see figure 2b) and the highest indexed percentage. This grain is therefore chosen for the monochromatic energy scan.

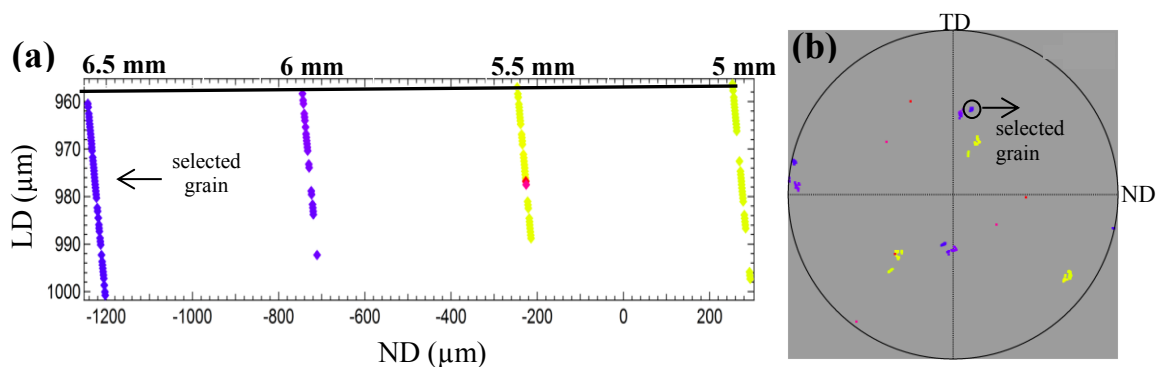


Figure 2. Grain orientations at different depths and different locations on the transverse surface (a) together with the corresponding $\{001\}$ pole figure (b). The grain selected for monochromatic energy scan for determination of lattice absolute spacing is marked. The black line in (a) marks the approximate position of the measurement surface. The colors in (a) and (b) correspond to the crystallographic orientations.

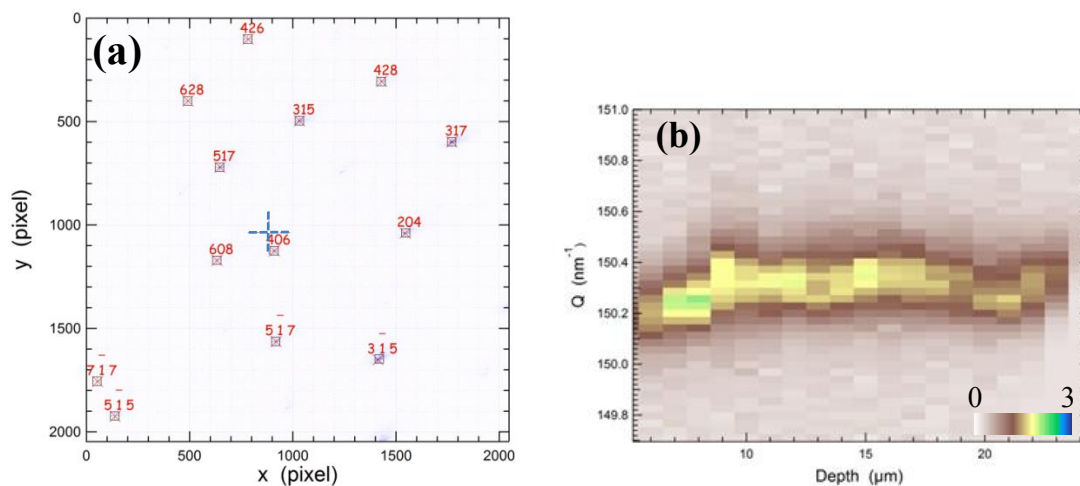


Figure 3. (a) Indexing of a polychromatic beam depth-resolved Laue diffraction pattern; (b) intensity distributions as a function of diffraction vector Q at each depth.

Figure 3a shows an indexed Laue pattern obtained at one of the depths from the polychromatic beam diffraction data for the selected grain, where the numbers indicate the assigned (hkl) indices of each spot. Based on this diffraction pattern the (517) spot was selected for monochromatic energy scanning,

as the intensity of this spot is relatively high and the corresponding X-ray energy is also high, at about 21 keV. The normal of the chosen (517) plane is about 2° away from sample normal direction, which is marked by the dashed cross in figure 3a.

From the monochromatic energy scan, the diffraction images around the (517) spot at each energy step for each depth were reconstructed. As each energy corresponds to a specific diffraction vector Q ($Q = 2\pi/d$), the integrated intensity of each diffraction image as a function of the diffraction vector can be determined at all X-ray penetration depths (see figure 3b). A few examples of the Q distribution at different depths are given in figure 4a, which clearly shows that the strain distribution varies within the measured volume from tensile to compressive strains. The dashed line marks the Q value corresponding to d_0 of the (517) crystallographic plane. A shift to the right relative to the dashed line indicates compressive strains and vice versa for tensile strains. At each depth, the Q distribution was fitted using a Gaussian function and the center of the distribution, Q_c was used to determine the crystallographic plane spacing, d .

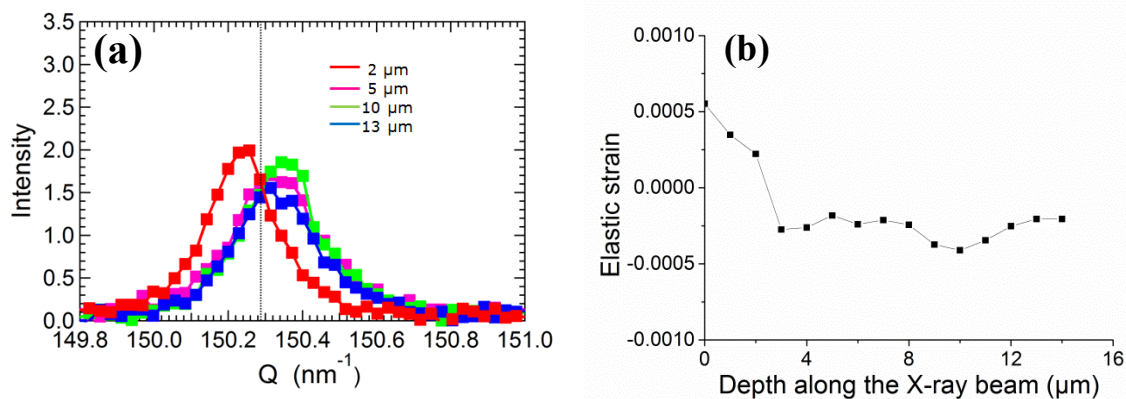


Figure 4. (a) Intensity variation as a function of Q at different depths within the sample (The dashed line marks the Q value for d_0 of the (517) crystallographic plane). (b) The residual strain along LD as a function of depth along the incoming X-ray.

Figure 4b shows the elastic strain component normal to the transverse surface of the sample developed in the nose crossing at different depths from the measuring surface. It can be seen that in the bulk of the material there are residual compressive strains in the range of 2×10^{-4} up to 4.11×10^{-4} .

Whereas theoretically the out-of-plane normal strain at a free surface is zero, tensile strains are seen within the first 3 μm from the free surface in figure 4b. Two explanations for this tensile strain are possible. Firstly, the reference d_0 may not be strain free. It is very likely that the grains even at depth of 20 mm below the running surface are also under compression, thus the dashed line in figure 4a should be shifted to the left, and the curve in figure 4b should move down towards more compressive strain. Secondly, due to small experimental errors, the free surface may be wrongly identified by about 2-3 μm from the currently assumed position. If the measurement surface in figure 4b (i.e. the 0 point) changes about 2-3 μm to the right, the tensile strain at the measurement surface is reduced. Irrespective of this, we can conclude the bulk of the measured volume is under compressive residual strains.

The problem of railway damage and failure can be caused by multiple mechanisms but it is evident that interaction between residual stresses and the defects (cracks etc.) can lead to severe problems. Generally compressive stresses are beneficial because they are supposed to inhibit crack propagation whereas tensile stresses are conducive for crack propagation. Although we find the longitudinal stresses are compressive, the normal or the transverse component of the stress may have a tensile component which could lead to crack evolution and failure. Also, generally the presence of a significant compressive stress is counterbalanced by a tension zone underneath. A complete map of all the components of the stresses in the three directions at different depths from the running surface

would be helpful to understand the interaction of residual stress with damage mechanisms. This will be investigated in future work. Also the synchrotron data will be compared with those measured using standard laboratory X-rays.

4. Conclusion

The residual strain distribution within a 5 mm thick slice of the nose of a manganese railway crossing was analyzed in the longitudinal direction at a distance of 6.5 mm from the rail surface. To our knowledge this is the first time synchrotron radiation has been employed to measure the strains in a nose of a manganese railway crossing. It was found that compressive strains exist along the longitudinal direction (with some small oscillations in the values) even at a depth of 6.5 mm from the wheel contact surface. Rail-wheel interactions at the nose of the crossing induces severe plastic deformation of the nose, the effect of which is thus evident even at a depth of 6.5 mm from the contact surface.

Acknowledgement

The authors gratefully acknowledge support from the Innovation Fund Denmark through the project “INTELLISWITCH – Intelligent Quality Assessment of Railway Switches and Crossings” (Grant no 4109-00003B) and grant from Interreg ESS & MAX IV: Cross Border Science and Society (Project number DTU-009). Use of the Advanced Photon Source was supported by the U.S Department of Energy, Office of Basic Energy Sciences, under Contract No.DE-AC02-06CH11357. The authors would also like to thank the Department of Materials and Manufacturing Technology at Chalmers University of Technology, Sweden for helping with the laboratory X-ray measurements.

References

- [1] Johansson A, Pålsson B, Ekh M, Nielsena JCO, Ander MKA, Brouzoulis J and Kassa E 2011 *Wear* **271** 472–481
- [2] Wiest M, Daves W, Fischer FD and Ossberger H 2008 *Wear* **265** 1431–38
- [3] Guo SL, Sun DY, Zhang FC, Feng XY and Qian LH 2013 *Wear* **305** 267-273
- [4] Lv B, Zhang M, Zhang FC, Zheng CL, Feng XY, Qian LH and Qin XB 2012 *Int J Fatigue* **44** 273-278
- [5] Harzallah R, Mouftiez A, Felder E, Hariri S and Maujean JP 2010 *Wear* **269** 647–654
- [6] Xiao JH, Zhang FC and Qian LH 2014 *Fatigue Fract Engng Mater Struct* **37** 219–226
- [7] Kaiser R, Stefanelli M, Hatzenbichler T, Antretter T, Hofmann M, Keckes J and Buchmayr B 2015 *J Strain Anal Eng* **50(3)** 190–198
- [8] Sasaki T, Takahashi S, Kanematsu Y, Satoh Y, Iwafuchi K, Ishida M and Morii Y 2008 *Wear* **265** 1402–07
- [9] Jun TS, Hofmann F, Belnoue J, Song X, Hofmann M and Korsunsky AM 2009 *J Strain Anal Eng* **44(7)** 563-568
- [10] Luzin V, Prask HJ, Herold TG, Gordon J, Wexler D, Rathod C, Pal S, Daniel W and Atrens A 2013 *Neutron News* **24(3)** 9-13
- [11] Rathod C, Wexler D, Luzin V, Boyd P and Dhanasekar M 2014 *Mater Sci Forum* **77** 213-218
- [12] Webster PJ, Hughes DJ, Mills G and Vaughan GBM 2002 *Mater Sci Forum* **404-407** 767-772
- [13] Pyzalla A, Wang L, Wild E and Wroblewski T 2001 *Wear* **251** 901–907
- [14] Kelleher JF, Buttle DJ, Mummery PM and Withers PJ 2005 *Mater Sci Forum* **490-491** 165-170
- [15] Kelleher J, Prime MB, Buttle D, Mummery PM, Webster PJ, Shackleton J and Withers PJ 2003 *J Neutron Res* **11(4)** 187-193
- [16] Liu W, Zschack P, Tischler JZ, Ice GE and Larson BC 2010 *AIP Conf. Proc.* **1365** 108-111
- [17] Tischler JZ 2014 Reconstructing 2D and 3D X-ray orientation map from white beam Laue *Strain and Dislocation Gradients from Diffraction* eds R Barabash and GE Ice (London: Imperial College Press) chapter 10 pp 358-375.